Received: 21 December 2020 | Revised: 20 April 2021 | Accepted: 9 May 2021

DOI: 10.1002/jmor.21382

RESEARCH ARTICLE

JOURNAL OF morphology WILEY

The filter-house of the larvacean *Oikopleura dioica*. A complex extracellular architecture: From fiber production to rudimentary state to inflated house

Khashayar Razghandi[1,2] | Nils Janßen[1] | Mai-Lee Van Le[3] | Thomas Stach[4]

[1]Biomaterials Department, Max Planck Institute of Colloids and Interfaces, Potsdam, Germany

[2]Cluster of Excellence "Matters of Activity. Image Space Material", Humboldt Universität zu Berlin, Berlin, Germany

[3]Institut für Biologie, AG Vergleichende Zoologie, Humboldt Universität zu Berlin, Berlin, Germany

[4]Institut für Biologie, AG Vergleichende Elektronenmikroskopie, Humboldt Universität zu Berlin, Berlin, Germany

Correspondence
Thomas Stach, Institut für Biologie, AG Vergleichende Elektronenmikroskopie, Humboldt Universität zu Berlin, Germany.
Email: thomas.stach@hu-berlin.de

Funding information
Deutsche Forschungsgemeinschaft

Abstract

While cellulose is the most abundant macromolecule in the biosphere, most animals are unable to produce cellulose with the exception of tunicates. Some tunicates have evolved the ability to secrete a complex house containing cellulosic fibers, yet little is known about the early stages of the house building process. Here, we investigate the rudimentary house of *Oikopleura dioica* for the first time using complementary light and electron microscopic techniques. In addition, we digitally modeled the arrangement of chambers, nets, and filters of the functional, expanded house in three dimensions based on life-video-imaging. Combining 3D-reconstructions based on serial histological semithin-sections, confocal laser scanning microscopy, transmission electron microscopy, scanning electron microscopy (SEM), and focused ion beam (FIB)-SEM, we were able to elucidate the arrangement of structural components, including cellulosic fibers, of the rudimentary house with a focus on the food concentration filter. We developed a model for the arrangement of folded structures in the house rudiment and show it is a precisely preformed structure with identifiable components intricately correlated with specific cells. Moreover, we demonstrate that structural details of the apical surfaces of Nasse cells provide the exact locations and shapes to produce the fibers of the house and interact among each other, with Giant Fol cells, and with the fibers to arrange them in the precise positions necessary for expansion of the house rudiment into the functional state. The presented data and hypotheses advance our knowledge about the interrelation of structure and function on different biological levels and prompt investigations into this astonishing biological object.

KEYWORDS
appendicularia, cellulose, extracellular matrix, filter, tunicata

1 | INTRODUCTION

Cellulose is the most abundant macromolecule in the biosphere (Heinze, 2016), giving red wood trees their stability and bacteria protection against predators. With its hierarchical structure, cellulose holds the potential to develop into a valuable, renewable technological material in numerous functional contexts (Li et al., 2021).

Multicellular animals however, are unable to produce cellulose with a single exception: tunicates also called urochordates (Ferrández-Roldán et al., 2019; Matthysse et al., 2004; Nakashima et al., 2004). The last common ancestor of this group of approximately 3000 marine invertebrate species evolved a cellulose synthase enzyme, probably through lateral gene transfer from a bacterium (Sagane et al., 2010). Tunicate cellulose is a major structural component molecule in the tunic, a more or less amorphous protective coat around the mostly sessile animals secreted by their epidermis (Hirose et al., 1999; Koo et al., 2002; Song et al., 2020; Zhao & Li, 2014). Among tunicates a few dozen species have evolved the ability to secrete a complex and intricate structure, that is, the house, constituting a multifunctional extracorporal architecture (Figure 1(a)).

Probably no other structure of animals embodies the multifarious functionalities of sophisticatedly combined carbohydrates and glycoproteins (Kimura et al., 2001; Kimura & Itoh, 2007; Riehl, 1993) like the appendicularian house. While the general internal structure and functional aspects of the appendicularian house are well documented (Flood, 1991, 2003, Deibel, 1986, Fenaux, 1986; an excellent review of the research history leading to our current functional understanding of appendicularian houses is found in Flood & Deibel, 1998—see further literature there), many details are still in need of exploration (see, e.g., Conley et al., 2018; Katija et al., 2020, Razghandi & Yaghmaei, 2020).

In the following paragraph, we give a brief summary of the functional morphology of the appendicularian house primarily following Flood and Deibel (1998) and Conley et al. (2018).

The house of appendicularians consists of a series of filters, chambers, channels, funnels, and valves (Lohmann, 1898, 1912, 1933, Fenaux, 1986, Conley et al. 2018; Figure 1). Water pumped through the system propels the animal through the plankton and is at the same time used in a filtration process that concentrates food particles by a factor of up to 1000 compared to the surrounding seawater (Flood, 1991; Knoechel & Steel-Flynn, 1989; Morris & Deibel, 1993). The driving force for water flow through the entire system is the animal's tail fitted into the tail chamber. Undulatory movement of the tail generates a pressure potential that sucks seawater laden with food particles from the outside through the laterally situated inlet filters (Alldredge, 1977, Flood, 1991; Figure 1). Coarse meshes prevent larger particles from entering the house. Water, together with smaller particles, is then directed via the short inlet funnels to the medially situated tail chamber. At the anterior end of the tail chamber the bilaterally symmetrical supply passages channel the water toward the entrance slots of the bilaterally symmetrical food concentration filter (Flood, 1991; Flood & Deibel, 1998). Here, food is concentrated by serial adhesion, when the upper and lower meshed membranes of the food concentration filter, the upper filter and the lower filter respectively entrap the food particles within the food concentration filter, upon tail rest (Conley et al., 2018). As the tailbeat stops, the slightly elastic house relaxes and the meshed membranes in the food concentration filter collapse on each other, resulting in accumulation of the food particles in between the two meshes while the filtered water passes through the meshes and into the posterior chamber. Upon resumed tail beat, the accumulated food is pulsed through elongated tubes of the food concentration traps, which merge into the food collecting tube. Eventually, food particles are conveyed through the mouth into the drawing stream generated by the cilia of the gill pores (Conley et al., 2018). During tail undulation, the increase of pressure in the posterior chamber results in the opening of the outlet valve of the house, and the produced stream propels the entire house with the animal inside through the water column (Alldredge, 1977, Flood, 1991, Flood & Deibel, 1998; Figure 1).

While these structural and functional components are comparatively well understood, only fragments of the secretion process

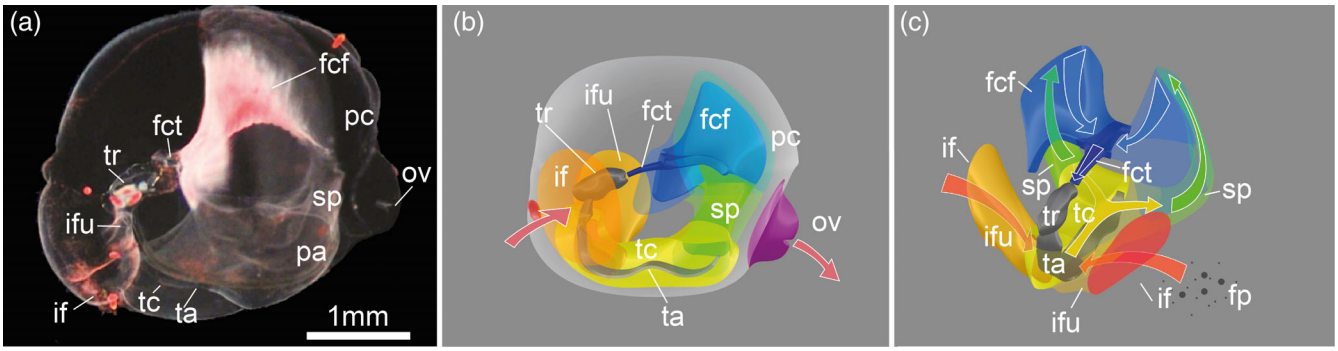

FIGURE 1 (a) *Oikopleura dioica*, individual inside the inflated filter-house. (A drop of milk and a needle tip of carmine powder were added to the sea water to visualize the otherwise transparent house). (b) Technical schematic 3D- representation of inflated filter-house. (c) As in panel (b), with the house membrane omitted and slightly tilted in order to better visualize the internal channeling and filtering system. **fcf**, food concentration filter; **fct**, food collecting tube; **fp**, food particles; **if**, inlet filter; **ifu**, inlet funnel; **ov**, outlet valve; **pc**, posterior chamber; **sp**, supply passage from tail chamber to fcf; **ta**, tail; **tc**, tail chamber; **tr**, trunk. Arrows indicate the waterflow through the filter-house. We use the same colors throughout the article to label identical structures

leading to such an extraordinarily complex structure have been described (Flood & Deibel, 1998; Lohmann, 1898; Sagane et al., 2010; Sagane et al., 2011; Spriet, 1997; Thompson et al., 2001) and the results of the most detailed treatment of this subject (Körner, 1952) are not compatible with a modern understanding of cellular mechanisms. For example, Körner described the secretion of fibers of the food concentration filter as a gradual condensation process within the Nasse cells, whereas the current model hypothesizes cellulose-synthase to be a transmembrane protein complex (Sagane et al., 2010; Sagane et al., 2011; Thompson et al., 2001). It is also obvious, that there has to be a coordination of the secretion process across the epithelium of the trunk on a molecular but also on a structural level, yet nothing is known about such a coordination.

Here, we investigate the structural arrangement of the rudimentary house in its uninflated stage of *Oikopleura dioica* for the first time using complementary microscopic techniques and supplement these studies with structural cellular and subcellular details of selected areas. In addition, we digitally modeled the arrangement of chambers, nets, and filters of the functional, expanded house in three dimensions based on life-video-imaging. By combining 3D-reconstructions based on serial histological semithin-sections, confocal laser scanning microscopy (CLSM), transmission electron microscopy (TEM), scanning electron microscopy (SEM), focused ion beam (FIB)-SEM, we were able to elucidate the precise arrangement of structural components, including cellulosic fibers, of the rudimentary house with an emphasis on the food concentration filter. We show that the folded rudiment of the appendicularian house is a precisely preformed structure with identifiable structural components intricately correlated with specific cells. During inflation, the rudimentary house increases by a factor of approximately 125x in volume and we suggest a model of how folded and inflated state can be linked in a coherent manner that is consistent with existing knowledge of internal channels and functioning of the system. In this model, the inferred processes of expansion and unfolding are predetermined by the arrangement and material characteristics of the secreted house and supported by the behavior of the animal.

In case the water flow through the expanded, functional house becomes obstructed, is compromised in another way or the animal is attacked by a predator, *Oikopleura dioica* can exit and discard the old house and replace it by a new one. A new house, already secreted and snugly fitting around the trunk in a sleeve-like fashion (Figure 2) is subsequently expanded. The expansion is at least partly aided by distinct movements of the animal, that eventually inserts the tail into the tail chamber while the expansion continues (Spriet, 1997). All fibers, membranes, and interconnected channels must be already produced in an elaborately folded, coherent, rudimentary pre-structure. The stereotypically patterned oikoplastic cells of the epithelium covering most of the animal's trunk are associated with the production and the precise arrangement of the filter meshes (Körner, 1952; Lohmann, 1933; Sagane et al., 2010; Sagane et al., 2011; Thompson et al., 2001).

Detailed descriptions and an elaborate nomenclature of the relative positions of the oikoplastic cells exist (Lohmann, 1933; Körner, 1952; Thompson et al., 2004; Kishi et al., 2017), and detailed observations of the distribution of oikosins, a highly diverse group of proteins are available (Sagane et al., 2010, Sagane et al., 2011, Thompson et al., 2001). However, very little is known about the structural arrangement of the rudimentary house and the ultrastructural morphology of the oikoplastic cells (Flood & Deibel, 1998). As mentioned above, what has been described in a classical light-microscopic formidable monographic publication on the secretion process (Körner, 1952) is at odds with the more modern understanding of cell biology such as the function of cellulose synthase molecules (Sagane et al., 2010, Sagane et al., 2011, Thompson et al., 2001).

By analyzing the microscopic and ultrastructural structure of oikoplastic cells and the rudimentary house, we provide a first sketch of the linkage between the molecular mechanisms described for the patterning of the oikoplastic epithelium (Sagane et al., 2010, Sagane et al., 2011, Thompson et al., 2001) and the functional understanding of the inflated house (Deibel, 1986; Fenaux, 1986; Flood, 1991, 2003; Flood & Deibel, 1998; Spriet, 1997).

2 | MATERIALS AND METHODS

2.1 | Life imaging

Living specimens of *Oikopleura dioica* were provided from Sars International Centre for Marine Molecular Biology (SICMMB) and cultured at Humboldt-University zu Berlin (HU) through numerous generations. Hundreds of movies ranging from 10 s to 3 min duration of animals moving normally within their inflated houses were recorded with a digital camera (Panasonic, Lumix DMC-LX7) mounted on the ocular tube of a dissecting microscope in 1920 × 1080/50p (PAL) AVCHD-progressive-format at SICMMB or HU. Animals were kept at ambient room temperature (20°C ± 2°C) in glass bowls of 15 cm diameter in filtered seawater of roughly 3 cm depth. A droplet of milk and a small amount of carmine powder were added to the artificial sea water in order to make internal structures of the transparent houses visible. These movies provided footage of inflated houses from all directions and allowed for a digital technical 3D-reconstruction of the house in its inflated state (see below).

2.2 | Fixation

For light microscopy animals were fixed either in Bouin's solution, an aqueous solution containing 8% formaldehyde, 5% acetic acid, and 1% picric acid, or in a cold solution of Karnovsky's primary fixative (Karnovsky, 1965), consisting of 2% glutaraldehyde, 2% paraformaldehyde, 1.52% NaOH and 1.2 g d-glucose, dissolved in 2.25% sodium hydrogen phosphate buffer (pH 7.4).

For electron microscopy, specimens were fixed for 1 h in a cold solution of Karnovsky's primary fixative (Karnovsky, 1965, see previous paragraph). Specimens were subsequently rinsed in three changes of buffer and post-fixed for 2 h in 1% OsO_4 solution at room temperature, dehydrated through a graded series of ethanol, and stored up to 6 weeks in 70% ethanol at 4°C.

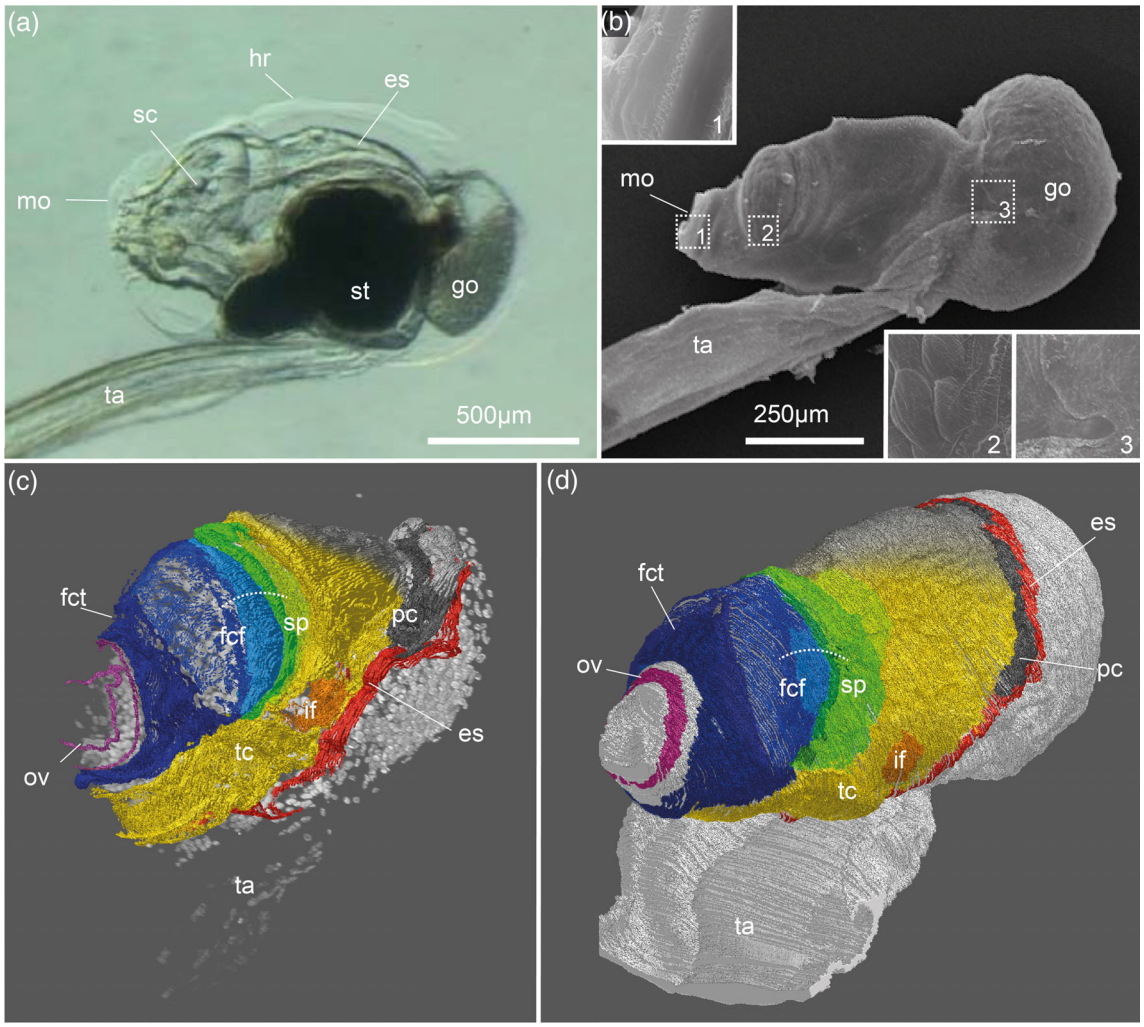

FIGURE 2 (a) *Oikopleura dioica*, dissecting-microscope image of a living sub-adult female individual of *Oikopleura dioica* after exiting the inflated house. Note the transparent thin house rudiment (**hr**) wrapped around the animals' trunk. (b) Scanning electron micrograph of an adult individual. The rudiment covers the animals' trunk anterior to the gonad. Magnified insets: 1—anterior ridge of the house rudiment, 2—food concentration filter and oikoplastic FoI domain, 3—posterior ridge of the house rudiment. Note the curved ridge that connects the house rudiment to the epidermis. (c & d) 3D reconstruction of rudimentary house based on confocal laser scanning microscopy and serial histological light microscopy respectively. The functional architecture and corresponding flow-path channeling sequence observed in the filtration process (Figure 1) is distinguished with the corresponding color coding in the folded house rudiment: escape slot (**es**, red), inlet filter (**if**, orange), tail chamber (**tc**, yellow), connecting to the supply passage (**sp**, lime/green), folded zone (turquoise), entrance slots and the upper transition zone of the food concentration filter (**fcf**, blue), lower transition zone, food collecting channel, food concentrating tube (**fct**, dark blue), and outlet valve (**ov**, purple). Dashed white line indicates the schematic sectional aspect in Figure 3(b) & Supporting Information S8. **go**, gonad; **mo**, mouth; **sc**, statocyst; **st**, stomach; **ta**, tail

2.3 | Confocal laser scanning microscopy (clsm)

Specimens were incubated in primary antibodies against tyrosinated α-tubulin (Anti-Tubulin, Tyrosine antibody produced in mouse; Sigma, St. Louis, Missouri, product number: T9028) for at least 2.5 days at 4°C. Incubation in secondary antibodies CyTM3 AffiniPure goat anti-mouse IgG (Jackson ImmunoResearch Laboratories, Inc., Philadelphia, Pennsylvania, code: 115-035-003) was carried out over night at room temperature; nuclei were labeled using 4′6-Diamidino-2-Phenylindole, Dihydrochloride (DAPI dihydrochloride, Thermo Fisher Scientific Inc., Waltham, Massachusetts, catalog number: D1306). Details can be found in Braun and Stach (2016). Every staining experiment was performed together with two different controls: one with primary antibodies omitted and the second with secondary antibodies omitted. Four specimens were examined in detail using a Leica TCS SPE confocal laser scanning microscope (Leica Microsystems, Heidelberg, Germany).

2.4 | Serial sectioning

Specimens for light microscopy were dehydrated in a graded series of ethanol and embedded in epoxy resin (Araldite; Fluka). Specimens were serially sectioned with a thickness of 0.5 µm–1 µm. Two specimens were serially sectioned for light microscopy (0.7 µm); another

specimen was serially sectioned alternating between 16 semithin sections (0.5 μm) and approximately 25 ultrathin sections (60 nm); one specimen was serially sectioned for transmission electron microscopy (60 nm). Sectioning was performed on a Leica Ultracut S. Semithin sections were stained using 1% toluidine blue in a solution of 1% sodium tetraborate (borax).

2.5 | Histology

Semithin sections stained with toluidine blue were digitally recorded using a Zeiss AxioCam HRc camera mounted on a Zeiss Axioscope 2 plus microscope at appropriate magnifications. Complete images were optimized for contrast and light balance using Adobe Photoshop CC Software. Images recorded from complete series of sections were used for 3D-reconstructions.

2.6 | Electron microscopy

For SEM, numerous specimens (approximately 50) were dehydrated in a graded series of ethanol and critical point dried in a Balzers Union CPD 030. Dried specimens were sputter coated with gold in a Balzers Union SCD 040 sputter coater and viewed with a LEO 1430. For TEM, ultrathin sections were stained with 2% uranylacetate and 2.5% lead citrate in an automatic stainer (courtesy of Dr. Björn Quast, Universität Bonn and Dr. Alexander Gruhl, MPI Bremen). Stained ultrathin sections were examined under a Zeiss EM9 transmission electron microscope, operated at 50 kV.

2.6.1 | Focused ion beam scanning electron microscopy

Focused ion beam milling and SEM (FIB-SEM) imaging were carried out with a ZEISS Crossbeam system (Crossbeam 540 Zeiss, Oberkochen, Germany) in order to acquire 3D-datasets with typical dimensions of $\sim 40 \times 30 \times 25\ \mu m^3$ with the pixel size of $\sim$39.97 nm. Prior to FIB-SEM imaging, the samples were carbon coated ($\sim$30 nm thickness) with vacuum carbon evaporator sputter coater (CED 030, Bal-tec/Balzers, Liechtenstein, Germany). The milling process was conducted with a gallium ion probe at 700 pA beam current and 30 kV acceleration voltage. This probe provided a slice thickness of 50 nm at a milling time of 5 s per slice. Secondary electron (SE) images were obtained with 2.5 kV acceleration voltage, 1 nA beam current and 21.6 s acquisition time per frame. Six specimens were used for FIB-SEM, and three of the resulting image stacks were used in digital 3D-reconstructions.

2.6.2 | Digital Three-Dimensional reconstructions

3D-models were created in Amira 5.4.3 (FEI Visualization Sciences Group, Berlin, Germany) based on the images of the serial semithin sections, the stacks of clsm, images, and the FIB-SEM recordings. Images were aligned in Amira. Using the "Segmentation Editor" mode of Amira, relevant structures were manually segmented on the stacked image data to generate a digital surface model. Additionally, the volume models were directly rendered from the clsm and FIB-SEM data using the "Volren" command.

Throughout this work, to follow the filtration flow path and correlate it to the underlying channeling structure in the folded rudimentary state, we assigned and followed a unified color code where the sequential shift in the rainbow's colors (red-orange-yellow-green-blue-purple) follows the water/particles path as it is circulated from outside the house membrane, through the inlet filter, in the tail chamber, and through the passages into the food concentration filter, collected toward the buccal tube, fed to the animal, excreted into the posterior chamber & pushed out of the outlet valve (e.g., Figure 1 (b,c)).

3 | RESULTS

3.1 | Structure of the rudimentary house

3.1.1 | General observations

In a first step, we identified the distinct regions described for the inflated house in the folded, rudimentary stage using different 3D-reconstruction techniques (see Figure 2). The rudiment of the house surrounds the anterior part of the trunk in a sleeve-like fashion with an anterior and posterior opening (Figure 2(a)). After the animal abandons an inflated house, the external (outer) house wall of the new rudiment can be seen lifted off of the epidermis, suggesting a swelling process (see also Flood & Deibel, 1998, Thompson et al., 2001; note that we are using descriptive terminology following the recommended terms listed in table 6.1 in Flood & Deibel, 1998, p. 108 with the sole exception of the term "oikoblastic" recommended there, where we stick to the more generally accepted "oikoplastic").

Different regions are recognizable in scanning electron micrographs of the house rudiment (Figure 2(b)). The rudiment is seen as a thin coat covering the animal's trunk, with the prospective outlet valve surrounding the mouth opening (Figure 2(b), inset 1) and a second, posterior opening, the prospective escape slot, fitted into an oblique groove just anterior to the gonadal swelling and passing ventrally immediately in front of the tail (Figure 2(b), inset 3). A smooth outer membrane, the external or outer house wall, covers the house rudiment completely. Immediately after secretion, the house rudiment envelops the major part of the trunk so tightly, that borders of neighboring epidermal cells can be discerned. This is more pronounced in the giant cells of Eisen's and Fol's oikoplast regions (Figure 2(b), inset 2).

Based on several microscopic techniques (confocal laser scanning microscopy, focused ion beam scanning electron microscopy, digital reconstructions based on series of semi-thin and ultra-thin sections for histological light and transmission electron microscopy), we

propose a model for the arrangement of the rudimentary house (Figures 2(c,d), Supporting Information S1, S3, S4, S5, S6, & S8). In doing so, several structures can serve as landmarks, that are identifiable with the applied techniques without difficulty and that can be readily related to the inflated functional state of the house. Such landmarks are the outlet valve, escape slot, the inlet filters, the food concentration filters, and the food collecting tube. Other structures can be inferred based on the microscopic data combined with the assumption of consistency with continuity of the water flow in the functional state, such as the passage, or the transition zones, or the tail chamber. While for the landmarks, structural details of the rudimentary state as well as cellular and subcellular details of the producing cells are described, descriptions of the latter group of structures are less definitive in our account.

3.1.2 | Landmark structure 1: Food concentration filter (fcf)

The most conspicuous structure of the oikoplastic epithelium is Fol's field consisting of seven Giant Fol cells and three rows of 26 Nasse cells immediately posterior to it (Figures 2(b) and 3, Supporting Information S2, S5, S7–S9). Using fluorescent stains in combination with confocal laser scanning microscopy, we could trace the origin of rectangularly arranged fibers in the food concentration filter of the rudimentary house to the apical surfaces of the three rows of Nasse cells (Figure 3(a–d), Supporting Information S2, S7–S9). Digital 3D-reconstructions of a complete series of semithin/ultrathin sections showed that the fibers emanating from the Nasse cells are tightly folded and packed in the narrow space between the apical cell surface and the external (outer) house wall (Figure 3(e,f), Supporting Information S2, S7–S9). Moreover, the close and intricate spatial association of the fibers, Nasse cells, and the row of seven Giant Fol cells is established. In order to analyze how the interrelation between Nasse cells and Giant Fol cells determines the arrangement of fibers in the fcf of the rudimentary house, we supplemented the confocal laser scanning microscopy with histological and ultrastructural investigations (see section *Cellular details and determination of fiber arrangement* below).

3.1.3 | Landmark structure 2: Inlet filter (if)

Eisen's field is another conspicuous area of cells, situated more ventrally and posteriorly to Fol's field (Figure 4, Supporting Information S10 & S11). Like Fol's field, Eisen's field consists of seven large cells, the Giant Eisen cells. These Giant Eisen cells are bordered by a row of 11 small cells at the anterior, ventral side. These small cells are called Chain of Pearl cells. Surrounding both, Giant Eisen cells and Chain of Pearl cells are Eisen's Yard cells (Figure 4(d), Supporting Information S10 & S11). Scanning electron micrographs show a conspicuous dome-shaped slightly elevated area of approximately 300 μm diameter. A row of 11 parallel knot-like protuberances is seen under the thin external (outer) house wall (Figure 4(c), Supporting Information S10 & S11). These rows span the entire area of Eisen's field, and are thus approximately 300 μm in length at a thickness of approximately 1 μm. 3D-reconstruction of the region of Eisen's field based on FIB-SEM milling, reveals that three of the Giant Eisen cells protrude in a mushroom-like fashion and with their apical parts cover the remaining four Giant Eisen cells (Supporting Information S10 & S11). In accordance with data from confocal laser scanning microscopy, the knot-like protuberances are found to be tightly spirally-coiled fibers that originate in a narrow fold formed between Giant Eisen cell 1 and the row of Chain of Pearl cells (Figure 4(d), Supporting Information S10 & S11).

3.1.4 | Landmark structures 3 & 4: Outlet valve and escape slot (ov, es)

These two structures are identified as the anterior and posterior ring-like openings that constitute the anterior and posterior rims of the house rudiment as it is covering the trunk of the animal. The anterior opening surrounds the mouth opening, the posterior opening fits into the epidermal groove passing dorsally anterior of the gonadal hump and ventrally just in front of anus and tail. Both opening structures in the house rudiment appear as conspicuous structures in confocal laser scanning micrographs that consist of ring-like bulges of either tightly folded or fibrous elements (Figures 2(c,d), 4(a), and 7(a)). While it seems logical to infer that the escape slot is eventually made up from the posterior opening in the rudimentary state of the house, this remains a tentative inference, because the exact structural nature and position of the escape slot in the functional, inflated house is basically unknown.

3.1.5 | Landmark structure 5: Food collecting tube (fct)

The food collecting tube is easily recognized in the serial histological sections and the confocal scanning micrographs (Figure 4(a), Supporting Information S1– S6). In the histological section the food collecting tube is seen as a dorsomedian anterior well-defined channel showing a light central appearance surrounded by thick, dark-stained material. Toward the posteriorly situated rudimentary food concentration filter, the food collecting tube bifurcates and continues into two lateral channel systems constituting the lower transition zone (see below). Confocal laser scanning micrographs also reveal the dorsomedian, anterior food collecting tube, as the comparatively thick walls are visible as wrinkled, folded, fibrous structures (Figure 4(a), Supporting Information S5, S6, & S8).

Between these landmark-structures, several other parts have to be present in the rudimentary house that are not so clearly distinguished, but that nevertheless can be described based on the microscopical investigations and the premise that the channeling-system in the rudimentary state corresponds to the one in the

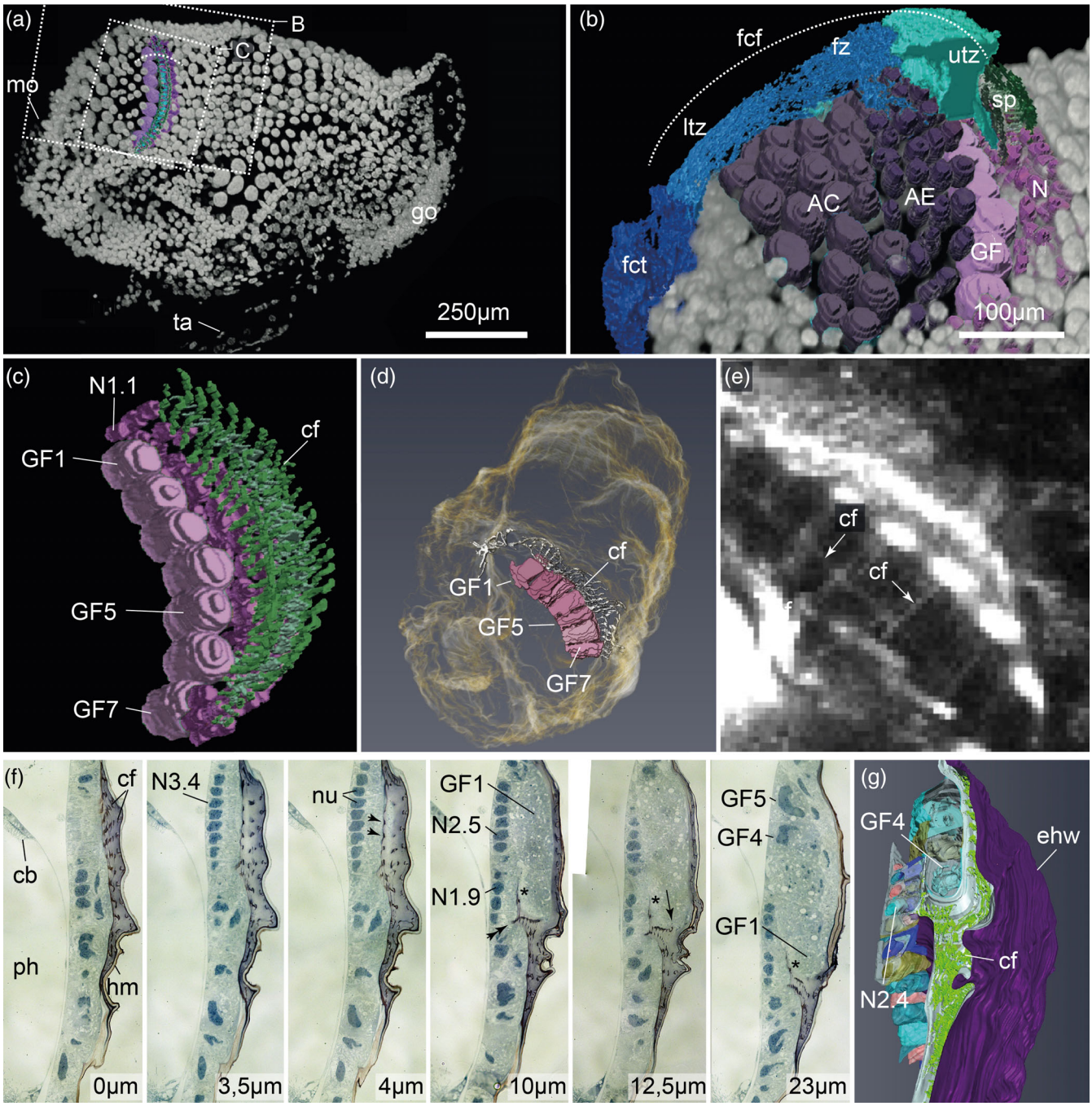

FIGURE 3 (a) *Oikopleura dioica*, confocal laser scanning micrograph of a sub-adult individual seen from the left; anterior is to the left (see also Figure 4(a)). z-Projection of the dapi channel of a complete stack of confocal laser scanning micrographs. The nuclei of cells of Fol's oikoplast region and apical fibers are segmented and highlighted. Dashed rectangles indicate areas magnified in panels (b) and (c), respectively. Dashed arced line indicates the schematic sectional aspect in Figure 3(b) & Supporting Information, Figure S8; see also Figure 2(c,e). (b) Enlarged area as indicated in panel (a) (see also Supporting Information S8). Segmented nuclei of cells in Fol's oikoplast region plus segmented fibers in the rudimentary house based on stacks of confocal images. (c) Enlarged area as indicated in panel (a). Segmented Giant Fol (**GF**) and Nasse (**N**) cells with fibers emanating from the Nasse cells. (d) Segmented Giant Fol cells (**GF**) and apical fibers superimposed on z-projection of the 519 nm-channel of a stack of confocal laser scanning micrographs, visualizing the house rudiment. (e) Higher magnification of the apical cellulosic fibers (**cf**) visible in a z-projection of the 519 nm-channel of a stack of confocal laser scanning micrographs. (f) Selected histological light micrographs (thickness 0.5 µm) from a complete series of sections from posterior to anterior. Numbers indicate distance from first section in the series. (g) 3D-reconstruction of cells, nuclei, fibers, and membranous structures of apically situated house rudiment in Fol's oikoplast region based on histological series, depicted in panel (f). **AC**, anterior crescent; **AE**, anterior elongated region; **cf**, cellulosic fibers; **cb**, ciliary band; **ehw**, external (outer) house wall; **fcf**, food concentration filter; **GF$_n$**, Giant Fol cell n; **go**, gonad; **mo**, mouth opening; **nu**, nucleus; **Nx.y**, Nasse cell y (counted from dorsal) in row x; **ph**, pharynx; **ta**, tail

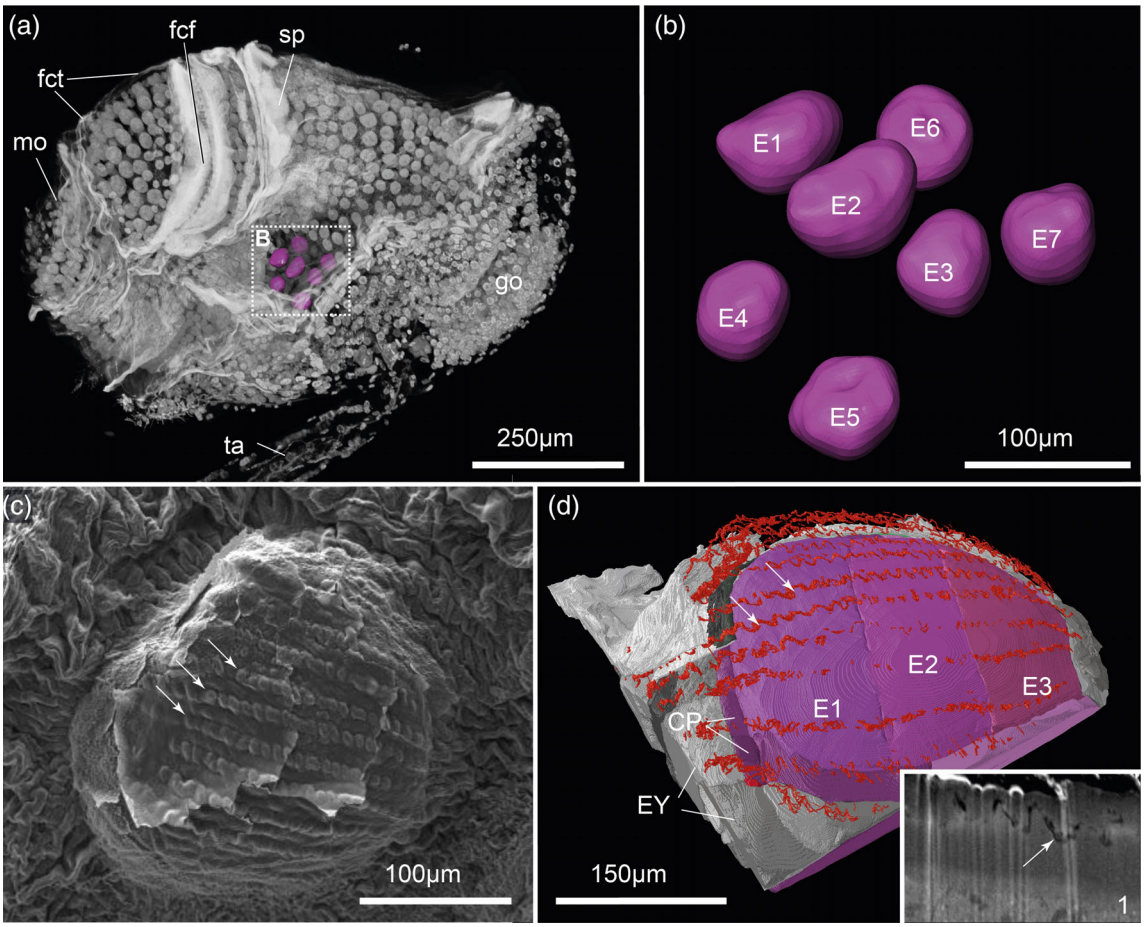

FIGURE 4 (a) *Oikopleura dioica*, confocal laser scanning micrograph of a sub-adult individual seen from the left; anterior is to the left (see also Figure 3(a)). z-Projection of the dapi and anti-acetylated tubulin channels of a complete stack of confocal laser scanning micrographs. The nuclei of the Giant cells of the oikoplastic Eisen domain are segmented and highlighted in purple. (b) Enlargement of highlighted (dashed rectangle) region of (a) showing segmented Giant Eisen cells (**E1-7**). (c) Scanning electron micrograph of the Eisen domain. Note the parallel lines of knots covered by the house membrane (arrows). (d) 3D-reconstruction of Giant Eisen cells (**E1-3**), chain of pearl cells (CP), and adjacent Eisen's yard cells (**EY**). Note that E1-3 completely cover the remaining Giant Eisen cells (E4-7; compare to (b)). Arrows point to spiral fibers spanning Eisen's field. Inset: Depicting exemplary FIB-SEM image used as the basis for the 3D-reconstruction. Arrow in inset points to the structure resulting in the reconstruction of one of the spirally coiled fibers shown with arrows in panel (d). **fcf**, food concentration filter; **fct**, food concentration tube; **go**, gonad; **mo**, mouth opening; **ta**, tail; **sp**, supply passage

inflated state and remains continuously connected throughout the inflation process.

3.1.6 | Tail chamber

In the serial histological sections, the tail chamber is easily recognized as a light-colored, almost empty appearing space surrounded by darker and denser appearing membranous structures (see Supporting Information S1). Higher magnification reveals irregular fibrous content of low density inside the tail chamber. Posteriorly, the spaces that constitute the tail chamber extend laterally toward Eisen's oikoplast regions on both sides. Stacks of clsm-images suggest that the rudimentary tail chamber of a given side continues dorsally further up turning into/and connecting to the supply passage and toward the food concentration filter and food collecting tube (see Supporting Information S1).

3.1.7 | Supply passage

Immediately posterior to the rudiments of the food concentration filters, denser areas in clsm-images can be recognized (Figure 4(a)). In their wrinkled appearance in clsm-images, these areas resemble reefed sail cloth that follows the outlines of Fol's field posteriorly. Dorsally and ventrally, the "reefed sail cloth" is folded back on itself on each side respectively (see also Figure 3(b), Supporting Information S2, S7, & S8).

3.1.8 | Upper transition zone

Connecting tail chamber, supply passage, and the food concentration filter is the upper transition zone. In the inflated house the supply passage leads to the upper end of the food concentration filter (Figure 1 (c)) via approximately rectangular entrance slots in the upper transition

zone (Thompson et al. (2001) illustrate the entrance slots clearly in a schematic drawing). In the rudimentary house this connection was tracked directly above Fol's oikoplast region containing the Giant Fol cells and Nasse cells. The upper transition zone is visible in consecutive serial histological sections as a narrow space ventrolaterally that is limited by denser membranes (Figures 3(b), Supporting Information S1, S2, S7–S9). The denser appearing membranes separate a dorsal from a more ventrally situated portion of the upper transition zone, indicating a sharp horizontal fold in the rudimentary upper transition zone (Supporting Information S2, S7–S9).

3.1.9 | Lower transition zone

The Lower transition zone connects the food concentration filter and the food concentrating tube. In consecutive histological sections the lower transition zone can be seen as a conspicuous area of hardly stained, relatively loose floccular material lined distally and proximally by denser membranes (Supporting Information S1 & S2). The external (outer) house wall constitutes the distally situated membrane of these two membranes. Dorsally, the lower transition zone connects to the lumen of the food concentrating tube via a narrow slit that is supported by denser membranous structures and equipped with a flap like vent. The entire Lower transition zone thus constitutes an obliquely elongated tube with clearly marked boundaries (Figure 3(b), Supporting Information S7 & S8).

3.1.10 | Escape chamber and posterior chamber

Two structures that have been described in the expanded house of appendicularians, the escape chamber and the posterior chamber, could not be identified with certainty. In the expanded house, the two structures are situated at opposite ends, the escape chamber at the front of the house (as defined by the direction of normal movement of the house), the posterior chamber at the abfrontal end. In the serial histological sections at the dorsal side, posterior in the animal an area of loose floccular material can be traced posteriorly just underneath a conical protuberance (Supporting Information S1). This conical dorsal protuberance is easily identified by the comparatively thick house membrane, the denser material filling the cone, and by the intensely stained spot that forms the tip of the cone (Supporting Information S1). This cone, likely secreted by the anterior rosette cells (Flood, 1994) probably constitutes the rudimentary bow of the expanded house, whereas the area of loose floccular material could correspond to the Escape chamber.

In the expanded house, the posterior chamber is situated between the food concentration filter from which it receives the filtered water and the exit valve from which superfluous water is expelled. It consists of two compartments, a more ventrally situated lower compartment and a dorsally situated upper compartment that connects to the upper transition zone. Anterior in the animal, median on its ventral side an area of loose floccular material is situated underneath the house membrane and a layer of more densely stained material (see supplementary online material). Slightly more posteriorly, a narrow area of light stained, loose floccular material can be seen ventrolaterally on both sides of the animal (Supporting Information S1). While the ventromedian anterior area of loose material according to its position and structure most probably constitutes the ventral compartment of the posterior chamber, the identification of the latter, more posteriorly situated areas as upper compartments remains more tentative.

3.2 | Cellular details and exemplary determination of local fiber arrangement in relation to the rudimentary house

In order to better understand cellular processes involved in the predetermination of the unfolded structural elements of the rudimentary house, we advanced the light-microscopical investigations of the Fol domain (see section *Landmarkstructure 1*: *Food concentration filter* above) using transmission electron microscopy. Digital 3D-reconstructions of fluorescent stained confocal laser scanning micrographs and complete series of semithin/ultrathin sections demonstrated that the fibers emanating from the Nasse cells are tightly folded and packed in the narrow space between the apical cell surface and the house membrane (Figure 3(e,f), Supporting Information S2, S5, S7–S9). Moreover, the close and intricate spatial association of the fibers, Nasse cells, and the row of seven Giant Fol cells was established.

Microscopical techniques utilizing fluorescent stains are limited by their capability to bind to specific antigens. Not detectable with fluorescent stains, the combined histological and TEM analysis revealed a narrow, crescent-shaped slit formed by the large Giant Fol cells bulging over the apical sides of the Nasse cells. Precisely spatially positioned transmission electron micrographs within the 3D-reconstructions could elucidate subcellular arrangements of fibers and interacting cells (Figure 5, Supporting Information S2, S5, S7–S9). Deep indentations of the apical surfaces of the Nasse cells of approximately 2 μm depth and about 2 μm diameter are the likely sites of production of the main fibers of the food concentration filters (Figures 5(c,d) and 6(b,g,h)). Here, roundish profiles of medium electron density and a diameter of approximately 20 nm can be seen in TEM (Figures 5(d) and 6(b,h)). The fibers seen in TEM above the apical sides of the Nasse cells have a thickness of approximately 0.4 μm in the uninflated state and probably correspond to suspensory fibers identified by Flood (1991); see also Conley et al., 2018). Thinner fibers (approximately 0.1 μm in thickness) are seen in a plane perpendicular to the suspensory fibers in the narrow space afforded between the overhanging part of the Giant Fol cells and the Nasse cells (Figure 5(c–f)). Both cell types are rich in rough endoplasmatic reticulum in these areas. The thin fibers clearly span across neighboring Nasse cells (Figure 5(e,f)), but it is not clear, where they originate. However, the presence of roundish profiles of medium electron density and a diameter of approximately 20 nm in the apical cell membrane of the Nasse

cells (Figures 5(f) and 6(b,h)) could correspond to the ones observed in the indentations where the suspensory fibers originate (see above). These roundish profiles could correspond to the cellulose synthase complexes hypothesized by Sagane et al. (2010). The appearance of small vesicles approximately 30 nm in diameter in the Giant Fol cells close to the cell membrane bordering the thin fibers (Figure 5(e)) is also of interest. These vesicles contain floccular material, slightly more electron dense and thus similar in appearance to the thin fibers. Finally, on the more posterior-distal part of the Giant Fol cells the cell membrane shows a remarkable pattern that closely correlates to likewise notable profiles of the fibers within the rudimentary house (Figure 6(f)). In these regions, the profiles of the cell membrane of the Giant Fol cells form a right-angled bend with more or less regularly appearing deeper indentations. While the right-angled bend is similar

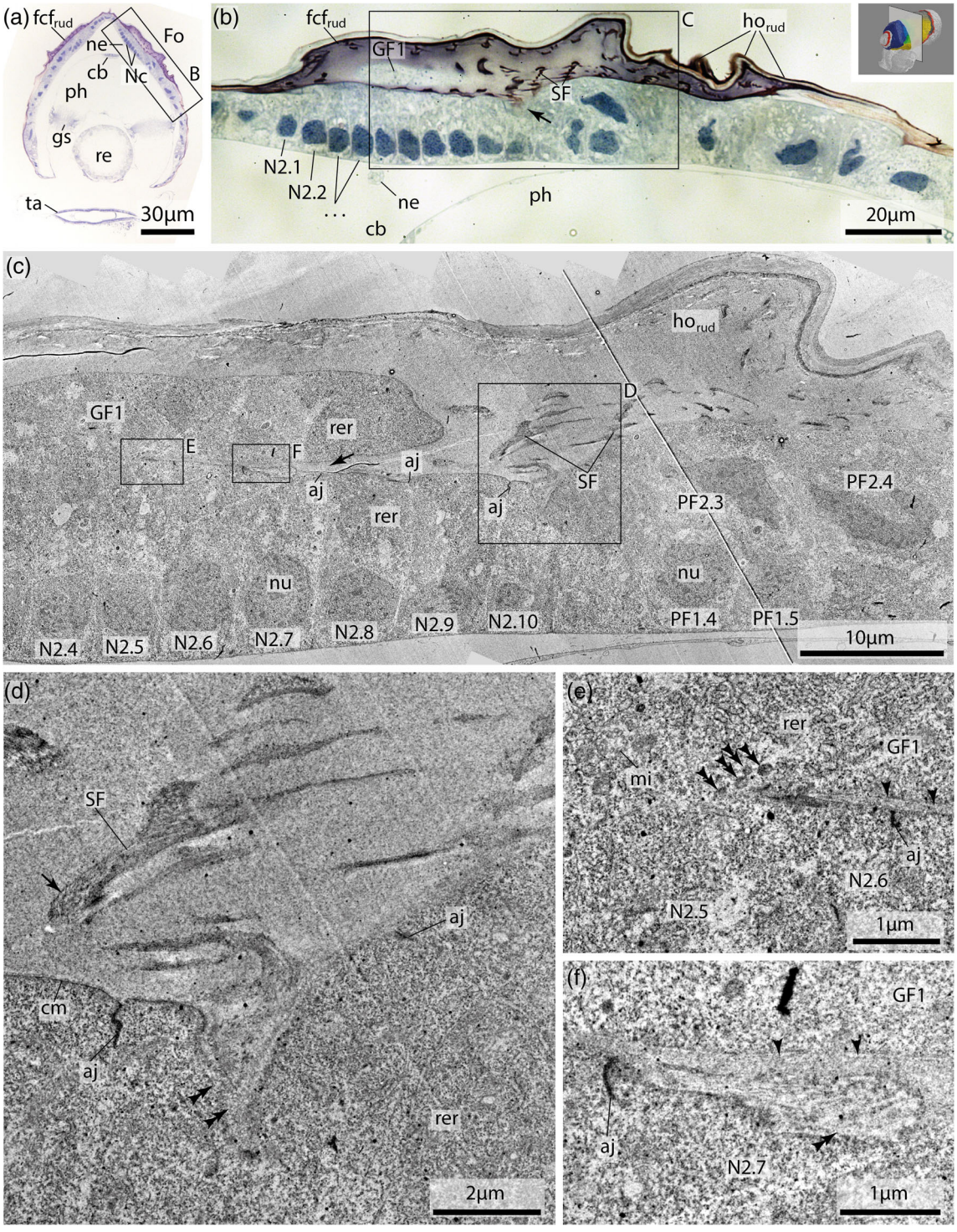

FIGURE 5 Legend on next page.

in shape and orientation to the ones observed in the nearby thicker fiber profiles, the number of deeper indentations corresponds to the number and approximate orientation of shorter fiber profiles associated with the thicker, angled fibers (Figure 6(f)).

Even within the area of Fol's field, TEM reveals diverse aspects of the intricate and highly structured appearance of the rudimentary house as well as details of the apical areas of the cells involved in the formation of the house (Figure 6). For example, the house rudiment is always distinctly layered with the outer house membrane appearing as a denser outer layer and other layers showing either floccular material or fine striations of electron denser lines indicating either potential for expansive swelling or alternatively dissolution in the former case or differential stress resistance in the latter (Figure 6(a–d)). Transmission electron micrographs also reveal that the darkly stained fibers in the histological preparations (Figures 3(e) and 5(b)), that likely contain cellulose, are made up of a denser fibrous core enveloped by a more floccular still fibrous material (Figure 6(c–e,g,h)). Grazing sections through cell membranes along the edges of sharp indentations in the apical cell membrane reveal batteries of round medium dense profiles of approximately 20 nm diameter on one side of the indentation and vesicles of approximately 40 nm diameter with slightly more electron dense, floccular material on the other side (Figure 6(g–i)). This structural assemblage concurs with the hypothesis that the dense fiber cores contain cellulose that is produced by cellulose synthase complexes in the apical membrane, that is, the 20 nm profiles of medium electron density in TEM, and that the floccular enveloping material contains proteinaceous material, perhaps oikosins, produced in the rough endoplasmic reticulum and transported to the apical membrane in small vesicles of 30–40 nm diameter.

4 | DISCUSSION

In summary, we reconstructed the rudimentary house as a cylindrical, sleeve-like structure snugly fitting around the trunk of the animal, with an anterior opening surrounding the mouth opening, a posterior opening anterior to the gonadal hump dorsally and ventrally anterior to the tail. Two more openings are marked by rather thick, spirally coiled fibers that form a coarse mesh—the inlet filters. Connecting the dots provided by the landmarks, our reconstruction places a continuous channel system in a shrunk, compressed, and folded manner inside the external (outer) house wall (see Figures 2 and 7).

Based on this reconstruction the inflation mechanism is inferred to constitute a complex process involving locally differential swelling, unfolding, expansion due to water pressure, but probably also confined areas of shrinkage (see Figure 7). For example, we infer that narrow, partly slit-like channels in the rudimentary house such as the tail chamber, the food concentrating tube, the posterior chamber, or the escape chamber need to expand considerably. Other structures such as the food concentration filter or the supply passage require unfolding and expansion simultaneously and in the case of the inlet filters expansion is accompanied by a despiralization of the fibers constituting the coarse filter net. This expansion process is partly supported by the inherent material characteristics of the rudimentary house, where hydration of sulfur-rich components and accompanied swelling have been demonstrated (Hosp et al., 2012). Water pressure generated by characteristic nodding movements of the trunk and specific undulatory movements of the tail additionally advance the expansion (Fenaux & Hirel, 1972; Spriet, 1997; Flood, 2003; Nakashima et al., 2011) and allows the animal to slip into the correct position of the expanded functional house. Because *Oikopleura dioica* has been developed into a model organism for molecular developmental studies (Bouquet et al., 2009; Seo et al., 2001; Spada et al., 2001), some molecular aspects of the house building process of the oikoplastic epithelial cells have been published.

Recently, Kishi et al. (2017) have investigated the ontogenetic pattern of cell divisions and movement that leads to the stereotypic arrangement of oikoplastic cells and presented a clear nomenclature for the individually recognizable cells based on the positions of nuclei that we adopt in the present study. In a pioneering study, Thompson et al. (2001) characterized specific expression domains of individual combinations of genes in the different oikoplastic fields among them the diverse and numerous oikosins, coding for the respective proteins. These proteins seem to be specific to appendicularians, because in a comparison between the genomes of *Oikopleura dioica* and *Ciona robusta* (then still called *C. intestinalis*, but see Brunetti et al., 2015, Pennati et al., 2015), Hosp et al. (2012) could not identify homologous genes in the *C. robusta* genome. However, the authors showed that

FIGURE 5 *Oikopleura dioica*, cellular and subcellular details within the oikoplastic Fol domain; see figurine in upper right corner for plane of section. (a) Light micrograph of a toluidine-blue stained cross section of complete animal. (b) Enlargement of region highlighted by a black rectangle in panel (a). (c) Transmission electron micrograph of adjacent section depicted in panels (a) & (b), corresponding to enlarged area indicated by rectangle in panel (b). Note slit (arrow) between Giant Fol (**GF1**) cell and apical sides of Nasse cells (**N2.y**). (d) Transmission electron micrograph. Higher magnification of the apical cell region of Nasse cells and adjacent fibers in the house rudiments indicated by black rectangle in panel (c). Note indentation of cell (double arrowheads) and fibrous material emerging from it. (e) Transmission electron micrograph. Higher magnification of the apical cell region of Nasse cells overarched by a Giant Fol cell (**GF1**); enlarged area indicated by black rectangle in panel (c). cell membranes are difficult to discern. Note fiber (single arrowheads) emerging from the area where three cells meet. Double arrowheads point to round structures of medium electron density. (f) Transmission electron micrograph. Higher magnification of the apical cell region of Nasse cells in contact with the overarching Giant Fol cell (**GF1**); enlarged area indicated by black rectangle in panel (c). The fiber shows a denser fibrous area (single arrowheads) and an area of more floccular, less dense appearance (double arrowhead). **aj**, apical junction; **cb**, ciliary band; **cm**, cell membrane; **fcf$_{rud}$**, rudimentary food concentration filter; **Fo**, Fol domain; **gs**, gill slit; **ho$_{rud}$**, house rudiment; **mi**, mitochondrion; **Nc**, Nasse cell; **ne**, nerve; **nu**, nucleus; **N2.x**, Nasse cell x in row 2; **PF2.x**, Posterior Fol cell x in row 2; **ph**, pharynx; **re**, rectum; **rer**, rough endoplasmic reticulum; **SF**, suspensory fibers; **ta**, tail

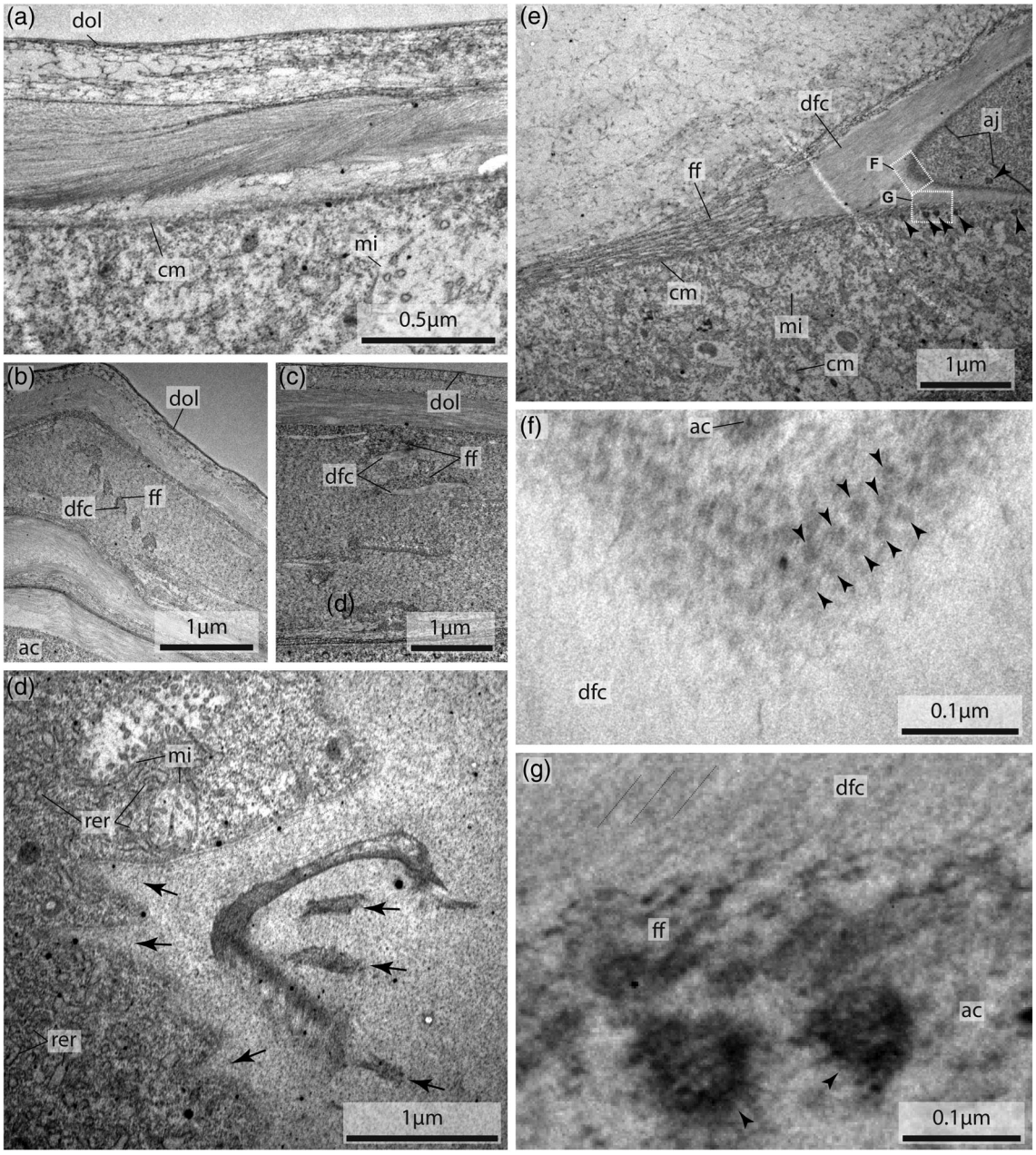

FIGURE 6 *Oikopleura dioica*, transmission electron micrographs depicting details of rudimentary house and apical cell regions of oikoplastic epithelium cells. (a) Region immediately anterior to Fol's oikoplast. Note the different striations visible in the rudimentary house layer. (b–g) Region of Fol's oikoplastic region showing arrangement of layers in the rudimentary house and the position of the suspensory fibers (b) consisting of a dense fiber core (**dfc**) and associated floccular fibers (**ff**) (c). (d) Cellular detail of a Giant Fol cell. Note the correspondence between the angle formed by the indentation in the apical cell surface and the main, bended suspensory fiber; note also the correspondence between the smaller but deeper indentations and the number of thinner, straight suspensory fibers (arrowheads). (e) Detail of apical area of three Nasse cells (approximately 9 µm posterior to the section depicted in Figure 5(d)). The material of the floccular fibers and the dense fiber core is seen closely adjacent to the apical cell surfaces. Note the electron dense structures close to the apical cell surfaces (arrowheads). White stippled rectangles outline areas enlarged in panels (f) and (g). (f) Magnified area indicated in panel (e). Grazing section along the cell surface shows regularly arranged structures of medium electron density (arrowheads). (g) Magnified area indicated in panel (e). Note the fine striation (thin stippled lines) in the dense fiber core (dfc); also, note that the floccular fibers (ff) are not clearly separable from the apical cytoplasm (ac). Arrowheads mark the electron dense structures immediately beneath the apical cell surface. **ac**, apical cytoplasm; **aj**, apical junction; **cm**, cell membrane; **dfc**, dense fiber core; **dol**, dense outer layer; **ff**, floccular fibers; **mi**, mitochondrion; **rer**, rough endoplasmic reticulum

the regional specific expression of the oikosins in the oikoplastic epithelium corresponds to spatially restricted presence of the corresponding oikosins in the house. Mikhaleva et al. (2018) showed that the expression of the approximately 80 known variants of oikosin genes in *O. dioica* is developmentally controlled by hox genes. Another component of the house, cellulose fibers were investigated in Eric Thompson's

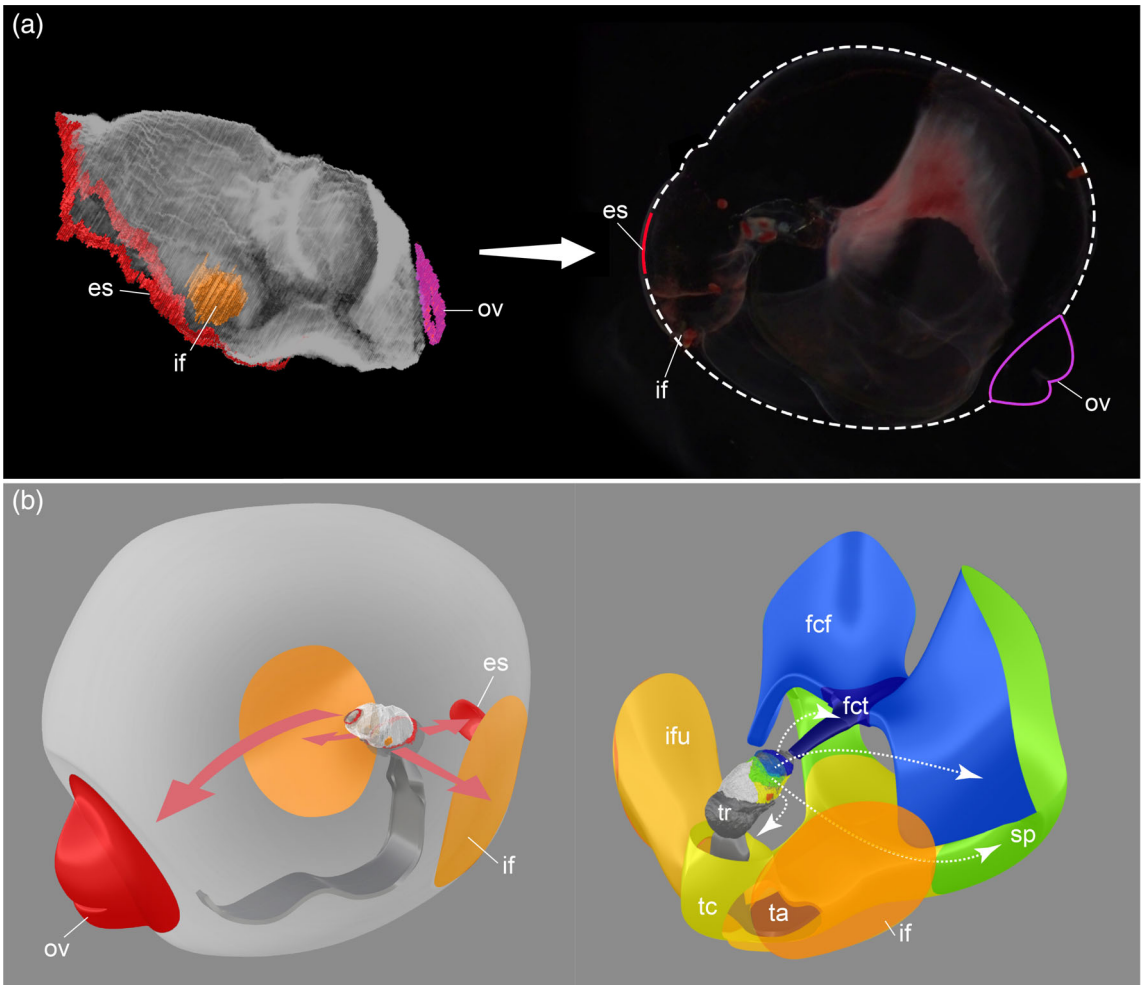

FIGURE 7 *Oikopleura dioica*, illustration of the inferred inflation process. (a) To the left, segmented data of the rudimentary house of *Oikopleura dioica* based on a stack of confocal laser scanning micrographs; openings in the house are marked by colors. Inlet filters (**if**, orange), outlet valve (**ov**, magenta) and escape slot (**es**, red). To the right, an individual of *Oikopleura dioica* inside the inflated filter-house is shown. (b) two aspects of a schematic representation of the inflated filter house of *Oikopleura dioica*. Arrows indicate the direction of expansion inferred for different structures in our study. Colors as in all other figures (see Figure 1 for color code). **es**, escape slot; **fcf**, food concentration filter; **fct**, food collecting tube; **if**, inlet filter; **ifu**, inlet funnel; **ov**, outlet valve; **sp**, supply passage from tail chamber to fcf; **ta**, tail; **tc**, tail chamber; **tr**, trunk

group and Sagane et al. (2010) showed that the gene coding for the cellulose synthase is duplicated in *O. dioica* compared to *C. robusta*: *Od-CesA1* (for *Oikopleura dioica*-Cellulose synthase A1) producing long fibers along the larval tail in *O. dioica* and *Od-CesA2* producing the cellulosic, fibrous scaffold of the house. Sagane et al. (2011) suggested, based on antibody labeling, that the cellulose synthase complexes in *O. dioica* are located in the apical cell membranes, similar to plant cells. However, different from plant cells they do not move along microtubules. Instead, the cellulose synthase complexes were suggested to be positioned by microtubules along a lattice of actin filaments. Almost nothing is known about the third obvious component, the viscoelastic mucus hydrogel, that probably constitutes a major part of the volume of the appendicularian house. Demouveaux et al. (2018) review some aspects pertinent to structure and function of gel-forming mucins and specifically mention *Oikosin-1* as a constituent part of the mucus in the house.

Linking this molecular level knowledge to higher structural levels has been attempted, yet little can be stated in this respect. We agree with the largely negative evaluation by Flood and Deibel (1998) of Körner's (1952) publication, which, although detailed, is at odds with the molecular and cellular details reviewed above and presented below. Flood and Deibel (1998) suggested some links between oikoplastic fields and structures of the functional house. Our evidence presented here is in general agreement with the findings of these authors, for example, in our reconstruction, the circumoral domain also produces the outlet valve, the ventro-lateral domain is likewise the area, where the tail chamber is produced, and the posterior keel of the house in our model is also produced by the anterior rosette. In these cases, we add information on the distinct positioning of the structures in the rudimentary house in situ. Different from Flood and Deibel (1998) our reconstruction regards the escape chamber and escape slot as produced by the unnamed cells that

posteriorly in the trunk are situated immediately in front of the ring that fastens the rudimentary house to the trunk. In this interpretation, the opening formed by the secretion process is providing the opening of the escape slot. The involvement of Fol's field in the production of the food concentration filter and of Eisen's field in the secretion of the inlet filter has been already reported in the classic treatises (Lohmann, 1933). Focusing our analyses on these higher structural levels allowed us to suggest how the identified structural elements are positioned and connected in the rudimentary house.

While the complex yet intricate house of appendicularians, is clearly integrated on all biological levels, the present study is to our knowledge the first investigating the microscopic structures involved in the formation of the house rudiment in an appendicularian since the light microscopic study by Körner (1952) that, as mentioned above and noticed before (Flood & Deibel, 1998), was limited by the technique as well as the cell biological concepts of its time. While we were able to document numerous microscopical details of the rudimentary house along with the three-dimensional arrangement of the components within the rudimentary house and suggest how these components expand and unfold in order to result in the functional, inflated house, it is clear that more questions remain unanswered. These range from questions regarding the fine-tuned material properties involved, to fundamental biological questions how secretion of such a complex intricate structure is coordinated between the hundreds of cells involved on a cellular and molecular level.

5 | CONCLUSION

Thus, based on our data we suggest that ultrastructural details of the apical surfaces of the cells (a) provide the exact locations and shapes to produce the fibers of the house and (b) interact among each other and with the fibers to arrange them in the intricate shape and precise positions necessary to enable the smooth and swift expansion of the rudimentary structure into the inflated and multifunctional house. While we are painfully aware that more questions remain open, we think that our study advances our knowledge about the interrelation of structure and function on different biological levels and will also prompt future investigations into this astonishing biological object.

ACKNOWLEDGMENTS

We would like to express our sincere gratitude to Dr. Katrin Braun, Peer Martin, and Sinah Pecina for their expert help and assistance in the laboratory and with the digital reconstructions. The authors acknowledge the support of the Cluster of Excellence at the Humboldt-Universität zu Berlin »Image Knowledge Gestaltung. An Interdisciplinary Laboratory« (EXC 1027/1) and support of the Cluster of Excellence »Matters of Activity. Image Space Material« (EXC 2025 – 390648296), both clusters funded by the Deutsche Forschungsgemeinschaft (DFG, German Research Foundation) under Germany's Excellence Strategy.

AUTHOR CONTRIBUTIONS

Khashayar Razghandi: Conceptualization; data curation; formal analysis; investigation; methodology; project administration; supervision; validation; visualization; writing-original draft; writing-review & editing. **Nils Janßen:** Data curation; formal analysis; software; visualization; writing-review & editing. **Mai-Lee Van Le:** Data curation; formal analysis; software; visualization; writing-review & editing. **Thomas Stach:** Conceptualization; data curation; formal analysis; funding acquisition; investigation; methodology; project administration; supervision; validation; visualization; writing-original draft; writing-review & editing.

PEER REVIEW

The peer review history for this article is available at https://publons.com/publon/10.1002/jmor.21382.

DATA AVAILABILITY STATEMENT

Data available as supplementary online material. Additional data available upon request from the authors.

ORCID

Thomas Stach https://orcid.org/0000-0001-5461-9069

REFERENCES

Alldredge, A. L. (1977). House morphology and mechanisms of feeding in the Oikopleuridae (Tunicata, Appendicularia). *Journal of Zoology*, *181*, 175–188.

Bouquet, J.-M., Spriet, E., Troedsson, C., Otterå, H., Chourrout, D., & Thompson, E. M. (2009). Culture optimization for the emergent zooplanktonic model organism *Oikopleura dioica*. *Journal of Plankton Research*, *31*, 359–370.

Braun, K., & Stach, T. (2016). Comparative study of serotonin-like immunoreactivity in the branchial basket, digestive tract, and nervous system in tunicates. *Zoomorphology*, *135*, 351–366.

Brunetti, R., Gissi, C., Pennati, R., Caici, F., Gasparini, F., & Manni, L. (2015). Morphological evidence that the molecularly determined *Ciona intestinalis* type A and type B are different species: *Ciona robusta* and *Ciona intestinalis*. *Journal of Zoological Systematics and Evolutionary Research*, *53*, 186–193.

Conley, K. R., Gemmell, B. J., Bouquet, J.-M., Thompson, E. M., & Sutherland, K. R. (2018). A self-cleaning biological filter: How appendicularians mechanically control particle adhesion and removal. *Limnology and Oceanography*, *63*, 927–938.

Deibel, D. (1986). Feeding mechanism and house of the appendicularian *Oikopleura vanhoeffeni*. *Marine Biology*, *93*, 429–436.

Demouveaux, B., Gouyer, V., Gottrand, F., Narita, T., & Desseyn, J.-L. (2018). Gel-forming mucin interactome drives mucus viscoelasticity. *Advances in Colloid and Interface Science*, *252*, 69–82.

Fenaux, R. (1986). The house of *Oikopleura dioica* (Tunicata, Appendicularia): Structure and functions. *Zoomorphology*, *106*, 224–231.

Fenaux, R., & Hirel, B. (1972). Cinétique du déploiement de la logette chez l'appendiculaire *Oikopleura dioica* Fol, 1872. *Comptes Rendus de l'Académie des Sciences, Paris*, *275*, 449–452.

Ferrández-Roldán, A., Martí-Solans, J., Cañestro, C., & Albalat, R. (2019). *Oikopleura dioica*: An emergent chordate model to study the impact of gene loss on the evolution of the mechanisms of development. In W. Twordzydlo & S. M. Bilinski (Eds.), *Evo-devo: Non-model species in cell and developmental biology* (pp. 63–106). Springer Nature Switzerland AG.

Flood, P. R. (1991). Architecture of, and water circulation and flow rate in, the house of the planktonic tunicate *Oikopleura labradoriensis*. *Marine Biology*, *111*, 95–111.

Flood, P. R. (1994). Appendicularian houses – Architectural wonders of the sea. In *Evolution of natural structures. Proceedings of the 3rd*

International Symposium Sonderforschungsbereich 230 (pp. 151–156). Universität Stuttgart and Universität Tübingen.

Flood, P. R. (2003). House formation and feeding behaviour of *Fritillaria borealis* (Appendicularia: Tunicata). *Marine Biology*, *143*, 467–475.

Flood, P. R., & Deibel, D. (1998). The appendicularian house. In Q. Bone (Ed.), *The biology of pelagic tunicates* (pp. 105–124). Oxford University Press.

Heinze, T. (2016). Cellulose: Structure and properties. *Advances in Polymer Science*, *271*, 1–52.

Hirose, E., Kimura, S., Itoh, T., & Nishikawa, J. (1999). Tunic morphology and cellulosic components of pyrosomas, doliolids, and salps (Thaliacea, Urochordata). *The Biological Bulletin*, *196*, 113–120.

Hosp, J., Sagane, Y., Danks, G., & Thompson, E. M. (2012). The evolving proteome of a complex extracellular matrix, the *Oikopleura* house. *PLoS One*, *7*(7), e40172.

Karnovsky, M. J. (1965). A formaldehyde-glutaraldehyde fixative of high osmolality for use in electron- microscopy. *The Journal of Cell Biology*, *27*, 137A.

Katija, K., Troni, G., Daniels, J., Lance, K., Sherlock, R. E., Sherman, A. D., & Robison, B. H. (2020). Revealing enigmatic mucus structures in the deep sea using DeepPIV. *Nature*, *583*, 78–82. https://www.nature.com/articles/s41586-020-2345-2.pdf

Kimura, S., Ohshima, C., Hirose, E., Nishikawa, J., & Itoh, T. (2001). Cellulose in the house of the appendicularian *Oikopleura rufescens*. *Protoplasma*, *216*, 71–74.

Kimura, S., & Itoh, T. (2007). Chapter 13. Biogenesis and function of cellulose in the tunicates. In R. M. Brown, Jr. & I. M. Saxena (Eds.), *Cellulose: Molecular and structural biology* (pp. 217–236). Springer.

Kishi, K., Hayashi, M., Onuma, T. A., & Nishida, H. (2017). Patterning and morphogenesis of the intricate but stereotyped oikoplastic epidermis of the appendicularian, *Oikopleura dioica*. *Developmental Biology*, *428*, 245–257.

Koo, Y.-S., Wang, Y.-S., You, S.-H., & Kim, H.-D. (2002). Preparation and properties of chemical cellulose from ascidian tunic and their regenerated cellulose fibers. *Journal of Applied Polymer Science*, *85*, 1634–1643.

Knoechel, R., & Steel-Flynn, D. (1989). Clearance rates of *Oikopleura* in cold coastal Newfoundland waters: A predictive model and its trophodynamic implications. *Marine Ecology Progress Series*, *53*, 257–266.

Körner, W. F. (1952). Untersuchungen über die Gehäusebildung bei Appendikularien (*Oikopleura dioica* Fol). *Zeitschrift für Morphologie und Ökologie der Tiere*, *41*, 1–53.

Li, T., Chen, C., Brozena, A. H., Zhu, J. H., Xu, L., Driemeier, C., Dai, J., Rojas, O. J., Isogai, A., Wågberg, L., & Hu, L. (2021). Developing fibrillated cellulose as a sustainable technological material. *Nature*, *590*, 47–56.

Lohmann, H. (1898). Das Gehäuse der Appendicularien, sein Bau, seine Funktion und Entstehung. *Schriften des Naturwissenschaftlichen Vereins für Schleswig-Holstein*, *11*(2), 347–407.

Lohmann, H. (1912). Die von Sekretfäden gebildeten Fangapparate im Tierreich und ihre Erbauer. Mitteilungen aus dem Naturhistorischen Museum in Hamburg. 30. Jg. (2. Beiheft zum Jahrbuch der der Hamburgischen Wissenschaftlichen Anstalten 30. Jahrgang 1912). (pp. 255–295).

Lohmann, H. (1933). Erste Klasse der Tunicaten. Appendiculariae. In T. Krumbach (Ed.), *Handbuch der Zoologie* (pp. 15–202). Walter de Gruyter.

Matthysse, A. G., Deschet, K., Williams, M., Marry, M., White, A. R., & Smith, W. C. (2004). A functional cellulose synthase from ascidian epidermis. *PNAS*, *101*, 986–991.

Mikhaleva, Y., Skinnes, R., Sumic, S., Thompson, E. M., & Chourrout, D. (2018). Development of the house secreting epithelium, a major innovation of tunicate larvaceans, involves multiple homeodomain transcription factors. *Developmental Biology*, *443*(2), 117–126.

Morris, C. C., & Deibel, D. (1993). Flow rate and particle concentration within the house of the pelagic tunicate *Oikopleura vanhoeffeni*. *Marine Biology*, *115*, 445–452.

Nakashima, K., Nishino, A., Horikawa, Y., Sugiyama, J., & Satoh, N. (2011). The crystalline phase of cellulose changes under developmental control in a marine chordate. *Cellular and Molecular Life Sciences*, *68*, 1623–1631.

Nakashima, Y. K. L., Satou, Y., Azuma, J.-I., & Satoh, N. (2004). The evolutionary origin of animal cellulose synthase. *Development Genes and Evolution*, *214*, 81–88.

Pennati, R., Ficetola, G. F., Brunetti, R., Caicci, F., Gasparini, F., Griggio, F., Sato, A. T., Kaul-Strehlow, S., Gissi, C., & Manni, L. (2015). Morphological differences between larvae of the *Ciona intestinalis* species complex: Hints for a valid taxonomic definition of distinct species. *PLoS One*, *10*(5), e0122879. https://doi.org/10.1371/journal.pone.0122879

Razghandi, K., & Yaghmaei, E. (2020). Rethinking filter: An interdisciplinary inquiry into typology and concept of filter, towards an active filter model. *Sustainability*, *12*, 7284.

Riehl, W. M. (1993). Elemental analyses of oikopleurids and factors affecting house production rate of *Oikopleura vanhoeffeni* (Tunicata, Appendicularia) in coastal Newfoundland waters. Master's Thesis. Memorial University of Newfoundland. Memorial University Research Repository (pp. 1-64). https://research.library.mun.ca/4143.

Sagane, Y., Zech, K., Bouquet, J.-M., Schmid, M., Bal, U., & Thompson, E. M. (2010). Functional specialization of cellulose synthase genes of prokaryotic origin in chordate larvaceans. *Development*, *137*, 1483–1492.

Sagane, Y., Hosp, J., Zech, K., & Thompson, E. M. (2011). Cytoskeleton-mediated templating of complex cellulose-scaffolded extracellular structure and its association with oikosins in the urochordate *Oikopleura*. *Cellular and Molecular Life Sciences*, *68*, 1611–1622.

Seo, H.-C., Kube, M., Edvardsen, R. B., Jensen, M. F., Beck, A., Spriet, E., Gorsky, G., Thompson, E. M., Lehrach, H., Reinhardt, R., & Chourrout, D. (2001). Miniature genome in the marine chordate *Oikopleura dioica*. *Science*, *294*, 2506.

Song, G., Delroisse, J., Schoenaers, D., Kim, H., Nguyen, T. C., Horbelt, N., Leclère, P., Hwang, D. S., Harrington, M. J., & Flammang, P. (2020). Structure and composition of the tunic in the sea pineapple *Halocynthia roretzi*: A complex cellulosic composite biomaterial. *Acta Biomaterialia*, *111*, 290–301.

Spada, F., Steen, H., Troedsson, C., Kallesøe, T., Spriet, E., Mann, M., & Thompson, E. M. (2001). Molecular patterning of the oikoplastic epithelium of the larvacean tunicate *Oikopleura dioica*. *The Journal of Biological Chemistry*, *276*, 20624–20632.

Spriet, E. (1997). Studies on the house building epithelium of Oikopleurid appendicularia (Tunicata): Early differentiation and description of the adult pattern of oikoplast cells. Candidata scientiarum thesis in cell and developmental biology. Department of Zoology, University of Bergen, Norway (pp. 1–57).

Thompson, E. M., Kallesøe, T., & Spada, F. (2001). Diverse genes expressed in distinct regions of the trunk epithelium define a monolayer cellular template for construction of the oikopleurid house. *Developmental Biology*, *238*, 260–273.

Zhao, Y., & Li, J. (2014). Excellent chemical and material cellulose from tunicates: Diversity in cellulose production yield and chemical and morphological structures from different tunicate species. *Cellulose*, *21*, 3427–3441.

SUPPORTING INFORMATION

Additional supporting information may be found online in the Supporting Information section at the end of this article.

How to cite this article: Razghandi, K., Janßen, N., Le, M.-L.V., & Stach, T. (2021). The filter-house of the larvacean *Oikopleura dioica*. A complex extracellular architecture: From fiber production to rudimentary state to inflated house. *Journal of Morphology*, *282*(8), 1259–1273. https://doi.org/10.1002/jmor.21382